TEMPERATURE CYCLING STUDIES ON METAL-SEMICONDUCTOR CONTACTS

Dr. MONISHA CHAKRABORTY

Assistant Professor, School of Bio-Science & Engineering, Jadavpur University, 188, Raja S. C. Mallik Road, Kolkata-700032, India.

ABSTRACT

In the present work, contact resistivity of metal-semiconductor (M-S) contact is determined, based on the values of ideality factor and barrier height which are obtained from the Current–voltage (I-V) characteristics of M-S contact. I-V characteristics of M-S contacts are recorded in dark condition at room temperature (300ºK) and for a temperature cycle in dark, comprising increasing and decreasing temperatures from 300ºK to 333ºK. Thin films of $Cd_{1-x}Zn_xTe$ of 1μm and 100nm thickness are the semiconductor materials fabricated on nickel coated glass substrates and plain glass substrates respectively for 'x' varying from 0.0567 to 0.2210. Nickel, Aluminium, Indium, Silver and Copper are the top contact points deposited on these films. The present paper has dealt with the estimation of optimum top metallic contact and optimum 'x' in $Cd_{1-x}Zn_xTe$ thin films with respect to temperature cycling studies.

Keywords **-** Barrier height, Contact resistivity, Ideality factor, Metal-Semiconductor (M-S) contact, Temperature cycling studies, $Cd_{1-x}Zn_xTe$ thin films.

I. INTRODUCTION

An ohmic contact between a metal and a semiconductor is defined by the negligible contact resistance relative to bulk and spreading resistance of the semiconductor. Fabrication of ohmic contact on the surface of semiconducting material is an art rather than science. Theoretical models and approaches for the extraction of contact resistance of metal-semiconductor (M-S) contacts are reported in [1-8]. A modified method is reported in [9] to determine the value of contact resistivity suitable for both single crystalline and polycrystalline materials.

In this paper, contact resistivity of metal-semiconductor (M-S) contacts is obtained from a mathematical model [10], based on the values of ideality factor and barrier height which are obtained from Current – voltage (I-V) characteristics of M-S contact, recorded in dark condition at room temperature (300ºK) and for a temperature cycle in dark, comprising increasing and decreasing temperatures from 300ºK to 333ºK. The theoretical formulation for the calculation of ideality factor (n) and barrier height (ϕ_b) are reported in [11]. Some studies on metallic contacts on II-VI compound semiconductors and effects of thermal cycling on their stability are reported in [12-16]. Several approaches to extract diode parameters are reported in [2, 17-18].

Cadmium Zinc Telluride (CZT) is a radiation detector material that provides new functionality and improved performance in single-photon emission computed tomography (SPECT) [19, 20]. Large array CZT detector is constructed by a group of researchers and this is reported to be one of the largest detectors constructed for small animal radionuclide imaging [21]. But CZT suffers from ohmic contact problems because of its high electron affinity and large work function. Nickel has large work function [22-23] and the possibility of Nickel to match with CZT has been reported in [24]. In this work, Nickel, Aluminium, Indium, Silver and Copper are chosen as the top contact points on these semiconducting films and the amongst these the best M-S contact has been identified with respect to temperature cycling studies. Owing to extensive research and industrial work conducted by teams of solid-state physicists, engineers and medical physicists, CdTe/CZT detectors are now widely used. CdTe/CZT-based surgery probes have large impact on patient management in surgical oncology. Excellent large-field of view modules have already been realized as reported in [25]. The performance of a CZT dual Positron Emission Tomography (PET), dedicated for breast cancer, is studied by a group of researchers and these are reported in [26]. Studies in [27] report on dedicated emission mammotomography with CZT imaging detector. Works are published in [28] where researchers fabricated metal-semiconductor-metal planar $Cd_{1-x}Zn_xTe$ detectors from large $Cd_{1-x}Zn_xTe$ single crystals. A comprehensive review of the material properties of $Cd_{1-x}Zn_xTe$, with varying zinc content, is reported in [29, 30]. The range of 'x' in $Cd_{1-x}Zn_xTe$ thin film lies preferably within $0.05 \leq$ 'x' ≤ 0.95 [30, 31].

In this work, proper methods are adopted to fabricate $Cd_{1-x}Zn_xTe$ thin films of 1μm and 100nm thickness and these are discussed in section II of this paper. The mathematical calculation for obtaining 'x' is discussed in section III of this paper. The mathematical model as reported in [10] to obtain contact resistivity of M-S contact based on the values of ideality factor and barrier height which are obtained from the Current–voltage (I-V) characteristics of M-S contact is briefly discussed in section IV of this paper. The values of contact resistivity of the M-S contacts in dark condition at room temperature (300ºK) and

for a temperature cycle in dark, comprising increasing and decreasing temperatures from 300ºK to 333ºK are discussed in section V of this paper. The significance of the results of this work is discussed in section VI of this paper. The work is concluded in section VII of this paper.

II. MATERIALS AND METHODS

In this work, physical deposition method is adopted to fabricate large area $Cd_{1-x}Zn_xTe$ thin films of 1µm and 100nm thickness. Surface cleaning of the substrate has predominant effect on the growth of the film on it. Thus prior to deposition, glass substrates are carefully cleaned. Commercially available glass slides of dimensions 23 mm x 37 mm x 1 mm are dipped in chromic acid for two hours. These are washed with detergent and finally ultrasonically cleaned with acetone before use.

In order to design the six different compositions of $Cd_{1-x}Zn_xTe$ thin films of 1µm and 100nm thickness, six different % ratio of the stack layer of ZnTe/CdTe is chosen and these are 20:80, 30:70, 40:60, 50:50, 60:40 and 70:30. For these six ratios of the stack layer of ZnTe/CdTe, six different values of 'x' are obtained. The mathematical detail is discussed with a sample calculation in section III of this paper.

For the film fabrication, 500W RF Sputtering unit has been used. ZnTe and CdTe targets are placed in the target holders of the RF sputtering unit. Plain glass and Ni-coated glass substrates are kept at the bottom of the target holder and temperature to the order of 373°K is maintained on the substrates. Argon gas is injected from outside and pressure of the order of 10^{-2} Torr has been maintained. At this pressure, the RF unit is energized and a power of 500W with a frequency of 13.56 MHz is applied between the target and the substrate. On application of this RF power the target gets energized and vapour of the target material produced deposits on the substrate. At the substrate temperature, the film gets crystallized and the thickness is dependent on the sputtering time. Both CdTe and ZnTe targets are sputtered sequentially and a stack layer of ZnTe/CdTe is thus obtained. The stack layer is then annealed in vacuum (10^{-5} Torr) for an hour at 573°K. Both Cadmium and Zinc tried to inter-diffuse among each other to get into a stabilized state. Applications of thermal energy initiate both cadmium and zinc inter-diffusion. However, the stoichiometric ratio of cadmium and zinc is not equal and as a result the film is formed in the form of $Cd_{1-x}Zn_xTe$. The value of 'x' decides whether the film is CdTe or ZnTe. Thickness and deposition time for CdTe and ZnTe layers for each composition of $Cd_{1-x}Zn_xTe$ films of 1µm thickness are tabulated in Table 1(a). Similarly, thickness and deposition time for CdTe and ZnTe layers for each composition of $Cd_{1-x}Zn_xTe$ films of 100nm thickness are tabulated in Table 1(b)

Circular dots of 2 mm diameter of Nickel, Aluminium, Indium, Silver and Copper contacts are deposited by Vacuum Evaporation technique onto the films. The contacts are then annealed for half an hour in vacuum (10^{-5} Torr) at 373°K. The layered structures of the fabricated films of 1µm and 100nm thickness for I-V characteristic studies are shown in Fig. 1(a) and Fig. 1(b) respectively.

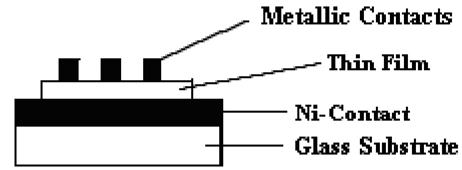

Fig. 1(a) Metal-Semiconductor structure for I-V characteristic studies for 1µm $Cd_{1-x}Zn_xTe$ thin film

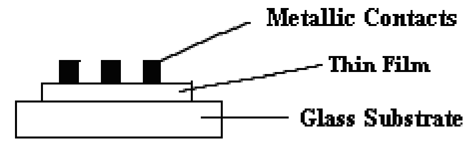

Fig. 1(b) Metal-Semiconductor structure for I-V characteristic studies for 100 nm $Cd_{1-x}Zn_xTe$ thin film

III. SAMPLE CALCULATION OF 'X'

In this section, the mathematics to determine 'x' in $Cd_{1-x}Zn_xTe$ thin film is discussed with a sample calculation. For this purpose, one out of the six samples is considered and this is a 1µm stack of CZT comprised of ZnTe film deposited on CdTe film. Percentage thickness ratio of ZnTe : CdTe layer is 60:40 and this can be expressed as given in Eq. (1.1).

$$\frac{\%ZnTe}{\%CdTe} = \frac{60}{40} = \frac{n_{ZnTe}}{n_{CdTe}} = \frac{\frac{m_{ZnTe}}{M_{ZnTe}}}{\frac{m_{CdTe}}{M_{CdTe}}} \tag{1.1}$$

where,
m_{ZnTe} and m_{CdTe} are the masses of ZnTe and CdTe layers respectively to attain the % ratio ZnTe : CdTe as 60:40.
M_{ZnTe} and M_{CdTe} are the molar masses of ZnTe and CdTe respectively and these values are M_{ZnTe} =193 gms/mol and M_{CdTe}=240 gms/mol. On putting these values, Eq. (1.1) becomes,

$$1.5 = \frac{\rho_{ZnTe}.T_{ZnTe}.A.240}{\rho_{CdTe}.T_{CdTe}.A.193} \tag{1.2}$$

where,
'A' is the cross-sectional area of the substrate. ρ_{ZnTe} and ρ_{CdTe} are the density of ZnTe and CdTe layers respectively and these values are ρ_{ZnTe} = 6.34 gms/cc and ρ_{CdTe}=5.85 gms/cc. T_{ZnTe} and T_{CdTe} are the values of thickness of ZnTe and CdTe layers respectively. On putting these values, Eq. (1.2) becomes,

$$\frac{T_{ZnTe}}{T_{CdTe}} = 1.113022477 \tag{1.3}$$

$$T_{ZnTe} + T_{CdTe} = 1\mu m \tag{1.4}$$

Solution of Eq. (1.3) and Eq. (1.4) gives the values of the thickness of CdTe and ZnTe layers and these are,
T_{CdTe} = 473.26 nm and T_{ZnTe} = 526.74 nm. (1.5 a)
Deposition rates for CdTe and ZnTe targets are 78 nm/min and 45 nm/min respectively. (1.5 b)
From Eq. (1.5 a) and Eq. (1.5 b) the deposition times for CdTe and ZnTe layers for this sample are obtained and these values are t_{CdTe} = 6 mins 4 sec and t_{ZnTe} = 11 mins 42 sec respectively. (1.5 c)
So, mass of ZnTe layer, $m_{ZnTe} = 3339.53.A.10^{-7}$ gms
and mass of CdTe layer, $m_{CdTe} = 2768.57.A.10^{-7}$ gms.
Molar mass of Zinc, M_{Zn} = 65.38 gms/mol.
So, $1139.29.A.10^{-7}$ gms of zinc is present in $3339.53.A.10^{-7}$ gms of ZnTe.
∴ Fraction of zinc in this CZT matrix

$$=\frac{1139.29.A.10^{-7}}{(2768.57+3339.53).A.10^{-7}}=0.1865 \quad (1.6)$$

Similarly, for other % ratios of ZnTe : CdTe layers for both the thickness domains considered in this study, the values of 'x' are calculated and these results are tabulated in Table 1(a) and Table 1(b).

IV. MATHEMATICAL MODEL

Contact resistivity (ρ_c) is given by,

$$\rho_c=\left(\frac{dV}{dJ}\right)_{V=0} \quad (1.7)$$

Normally, the J-V relationship of a rectifying contact is represented by

$$J=J_0[\exp(\frac{qV}{nKT})-1] \quad (1.8)$$

with V as applied voltage, Jo as reverse saturation current density, A_{eff} as effective area of M-S contact, n as ideality factor [23], T as absolute temperature (300°K), K as Boltzmann Constant [23]. Taking only the linear terms, and from Eq. (1.7) and Eq. (1.8),

$$\rho_c=\left(\frac{Aeff.n.K.T}{Io.q}\right) \quad (1.9)$$

Considering that the conduction has taken place at the metal-semiconductor interface due to thermionic emission phenomenon then,

$$I_0=Aeff.A^*.T^2.\exp\left(-\frac{q\phi_b}{kT}\right) \quad (1.10)$$

with ϕ_b as potential barrier at the metal-semiconductor interface, A^* as Richardson's constant=$1.20173*10^6 Am^{-2}K^{-2}$.
From Eq. (1.9) and Eq. (1.10),

$$\rho_c=\left(\frac{K.\exp\left(\frac{q\phi_b}{kT}\right)}{q.A.T}\right) \quad (1.11)$$

Where, $A=\left(\frac{A^*}{n}\right)$, (1.12)

ρ_c is evaluated using Eq.(1.11) where, n and ϕ_b are calculated using the theoretical formulation reported in [11] and it is briefly mentioned here.
In the equilibrium condition of a metal-semiconductor contact, the total current density (J) becomes,

$$J=J_0\left[\exp\left(\frac{qV_d}{nkT}\right)-1\right] \quad (1.13)$$

Where $V_d=V-JA_{eff}R_s$ and A_{eff} & R_s are the effective contact area and series resistance of the metal-semiconductor contact respectively.
J is the sum of two current components – from the semiconductor to the metal ($J_{S\to M}$) and from the metal to the semiconductor ($J_{M\to S}$), where

$$J_{S\to M}=J_0\exp\left(\frac{qV_d}{nkT}\right)$$

and $J_{M\to S}=J_0$

Here $$J_0=A^*T^2\exp\left(-\frac{q\phi_b}{kT}\right) \quad (1.13a)$$

At large forward bias (V_d>3kT/q), Eq.(1.13) reduces to,

$$J=J_0\left[\exp\left(\frac{qV_d}{nkT}\right)\right] \quad (1.13b)$$

On substituting the expression for V_d, Eq. (1.13b) becomes;

$$V=\frac{n}{\beta}\ln\left(\frac{J}{J_0}\right)+JA_{eff}R_s \quad (1.14)$$

Where, $\beta=\frac{q}{kT}$

Substitution of J_0 from Eq. (1.13a) in Eq. (1.14) gives,

$$V=JA_{eff}R_s+n\phi_b+\frac{n}{\beta}\ln\left(\frac{J}{A^*T^2}\right) \quad (1.15)$$

On differentiating V with respect to J, Eq. (1.15) reduces to,

$$\frac{dV}{dJ}=A_{eff}R_s+\frac{1}{J}\frac{n}{\beta} \quad (1.16)$$

The term $\frac{dV}{dJ}=R_D$, the dynamic resistance of the barrier.
A plot of R_D vs $\frac{1}{J}$ of Eq. (1.16) bears a straight line with $A_{eff}.R_s$ as the intercept and $\frac{n}{\beta}$ as the slope.
Again Eq. (1.15) can be rewritten as,

$$H(V)=JA_{eff}R_s+n\phi_b \quad (1.17)$$

Where $H(V) = V - \frac{n}{\beta}\ln\left(\frac{J}{A^*T^2}\right)$ (1.17a)

The values of H(V) can be evaluated by substituting values of J with corresponding values of V. Again the plot of H(V) vs. J bears a straight line with $A_{eff}R_s$ as the slope and $n\phi_b$ as intercept. From the above two plots the values of n and ϕ_b are evaluated.

V. RESULTS

Current-Voltage (I-V) characteristic data are recorded for all the M-S contacts using Keithley (Model No. 2440) 5A Source meter at room temperature of 300ºK in dark condition and for a temperature cycle in dark, comprising increasing and decreasing temperatures from 300ºK to 333ºK. Thin films of $Cd_{1-x}Zn_xTe$ of 1µm and 100nm thickness are the semiconductor materials fabricated on nickel coated glass substrates and plain glass substrates respectively for ‘x’ varying from 0.0567 to 0.2210. Nickel, Aluminium, Indium, Silver and Copper are the top contact points deposited on these films. Plots of R_D vs 1/J are obtained for all the M-S contacts and from these plots, the values of ideality factors (n) for these M-S contacts are calculated as discussed in section IV of this paper. Plots of H(V) vs. J are obtained for all the M-S contacts and from these plots, the values of barrier heights (Φ_b) for these M-S contacts are calculated as discussed in section IV of this paper. Substituting the values of ‘n’ and ‘Φ_b’ in Eq. (1.11), contact resistivity of these M-S contacts are evaluated. The effective area of these M-S contacts is 0.0314 cm^2.

Plots of normalized values of contact resistivity, ρ_{dt} vs thermal cycle comprising increasing and decreasing temperatures from 300ºK to 333ºK in dark with Nickel and Aluminium as metallic contacts on 1µm $Cd_{1-x}Zn_xTe$ thin film for ‘x’ varying from 0.0567 to 0.2210 are shown in Fig. 2(a), Fig.2 (b), Fig. 2(c), Fig. 2(d), Fig. 2(e), Fig. 2(f), Fig. 3(a), Fig.3 (b), Fig. 3(c), Fig. 3(d), Fig. 3(e) and Fig. 3(f) as sample results.

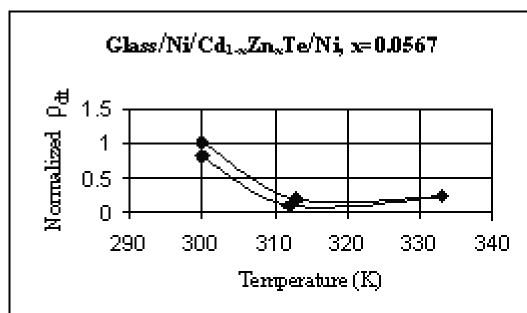

Fig. 2(a) Temperature Cycling of Nickel contact on $Cd_{1-x}Zn_xTe$ 1µm thin film at ‘x’ = 0.0567

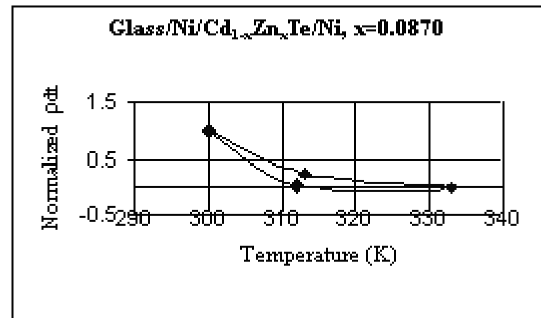

Fig. 2(b) Temperature Cycling of Nickel contact on $Cd_{1-x}Zn_xTe$ 1µm thin film at ‘x’ = 0.0870

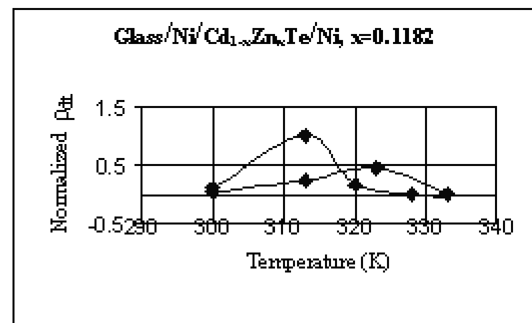

Fig. 2(c) Temperature Cycling of Nickel contact on $Cd_{1-x}Zn_xTe$ 1µm thin film at ‘x’ = 0.1182

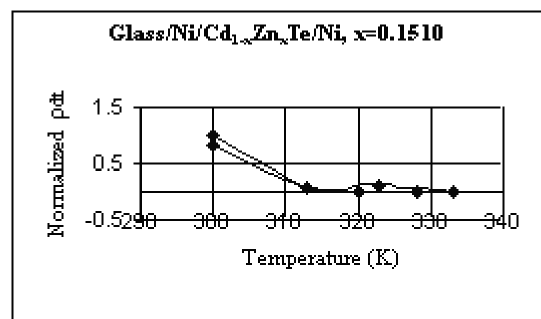

Fig. 2(d) Temperature Cycling of Nickel contact on $Cd_{1-x}Zn_xTe$ 1µm thin film at ‘x’ = 0.1510

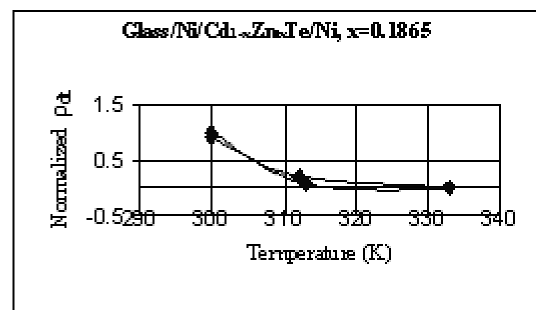

Fig. 2(e) Temperature Cycling of Nickel contact on $Cd_{1-x}Zn_xTe$ 1µm thin film at ‘x’ = 0.1865

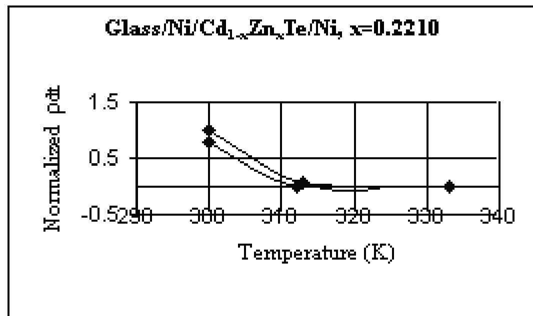

Fig. 2(f) Temperature Cycling of Nickel contact on $Cd_{1-x}Zn_xTe$ 1μm thin film at 'x' = 0.2210

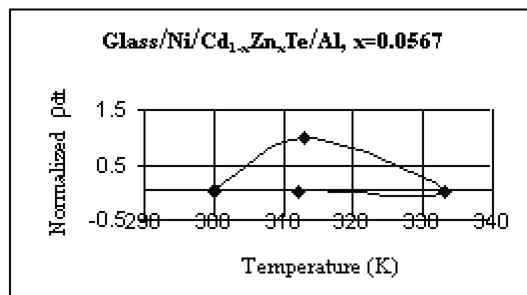

Fig. 3(a) Temperature Cycling of Aluminium contact on $Cd_{1-x}Zn_xTe$ 1μm thin film at 'x' = 0.0567

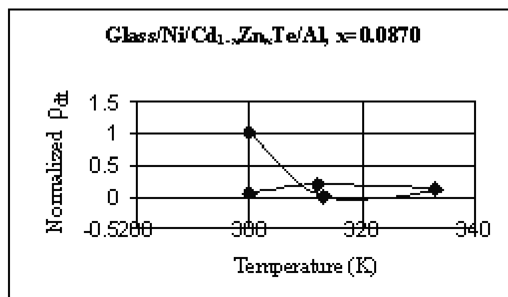

Fig. 3(b) Temperature Cycling of Aluminium contact on $Cd_{1-x}Zn_xTe$ 1μm thin film at 'x' = 0.0870

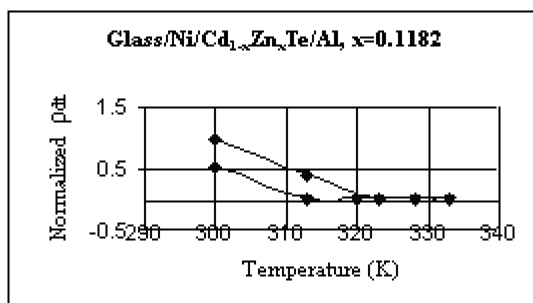

Fig. 3(c) Temperature Cycling of Aluminium contact on $Cd_{1-x}Zn_xTe$ 1μm thin film at 'x' = 0.1182

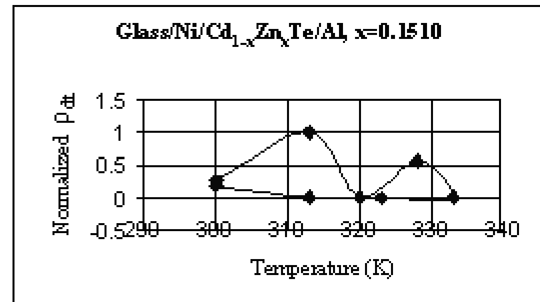

Fig. 3(d) Temperature Cycling of Aluminium contact on $Cd_{1-x}Zn_xTe$ 1μm thin film at 'x' = 0.1510

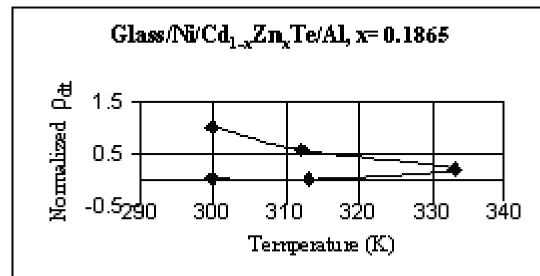

Fig. 3(e) Temperature Cycling of Aluminium contact on $Cd_{1-x}Zn_xTe$ 1μm thin film at 'x' = 0.1865

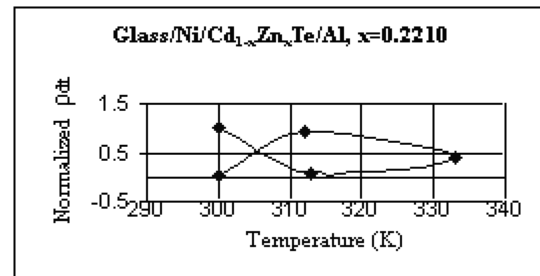

Fig. 3(f) Temperature Cycling of Aluminium contact on $Cd_{1-x}Zn_xTe$ 1μm thin film at 'x' = 0.2210

Similarly, for other metallic contacts on $Cd_{1-x}Zn_xTe$ 1μm thin films, plots of normalized values of contact resistivity, ρ_{dt} vs thermal cycle are obtained. From all these plots, it is observed that out of all the metallic contacts, e.g. Nickel, Aluminium, Indium, Silver and Copper deposited on all the six different compositions of $Cd_{1-x}Zn_xTe$ 1μm thin films, the forward and return paths of Nickel are the closest to each other in almost all the cases. So, it can be inferred that Nickel has the best thermal stability and this is an essential feature for ohmic contact.

On the basis of the above results, Nickel is chosen as the top metallic contact points on $Cd_{1-x}Zn_xTe$ 100 nm thin films. Samples are heated to 333°K and then they are allowed to cool to room temperature of 300°K. In dark condition, at room temperature of 300°K, the M-S contact performance parameters are ideality factor (n_d), barrier height (Φ_{bd}) and contact resistivity (ρ_d) as tabulated in Table 2. Similarly, after a temperature cycle in dark, comprising increasing and decreasing temperatures from 300°K to

333ºK the M-S contact performance parameters are ideality factor (n_t), barrier height (Φ_{bt}) and contact resistivity (ρ_{dt}) as tabulated in Table 2. The normalized values of the ratio ρ_{dt} / ρ_d are evaluated for these M-S contacts and these are tabulated in Table 2.

Out of the six compositions of $Cd_{1-x}Zn_xTe$ 100 nm thin films, three compositions have given good results and the normalized Nickel contact performance parameters for these three $Cd_{1-x}Zn_xTe$ 100 nm thin films in dark and after a temperature cycle in dark, comprising increasing and decreasing temperatures from 300ºK to 333ºK are tabulated in Table 2. It is observed from these results that the M-S contact performance parameters are functions of 'x'. The values of the ratio ρ_{dt} / ρ_d for all these three compositions of $Cd_{1-x}Zn_xTe$ 100 nm thin films with Nickel as the contact points are normalized with respect to the value of the ratio ρ_{dt} / ρ_d of $Cd_{1-x}Zn_xTe$ 100 nm thin film at 'x' = 0.1510 as tabulated in Table 2. From Table 2, it is observed that out of all these three compositions of $Cd_{1-x}Zn_xTe$ 100 nm thin films, with Nickel as the metallic contact points, the maximum decrease in the value of the ratio ρ_{dt} / ρ_d is found at 'x' = 0.1865.

Table 1(a) Thickness and Deposition Times of ZnTe and CdTe layers in 1μm CZT Films

S. No.	(%ZnTe):(%CdTe)	Thickness of ZnTe layer T_{ZnTe} (nm)	Thickness of CdTe layer T_{CdTe} (nm)	Deposition time of CdTe layer t_{CdTe}	Deposition time of ZnTe layer t_{ZnTe}	Fraction of Zinc in CZT matrix, 'x'
1	20:80	156.48	843.52	10 mins 49 sec	3 mins 29 sec	0.0567
2	30:70	241.29	758.71	9 mins 44 sec	5 mins 22 sec	0.0870
3	40:60	330.97	669.03	8 mins 35 sec	7 mins 21 sec	0.1182
4	50:50	425.95	574.05	7 mins 22 sec	9 mins 28 sec	0.1510
5	60:40	526.74	473.26	6 mins 4 sec	11 mins 42 sec	0.1865
6	70:30	633.88	366.12	4 mins 42 sec	14 mins 5 sec	0.2210

Table 1(b) Thickness and Deposition Times of ZnTe and CdTe layers in 100 nm CZT Films

S. No.	(%ZnTe):(%CdTe)	Thickness of ZnTe layer T_{ZnTe} (nm)	Thickness of CdTe layer T_{CdTe} (nm)	Deposition time for CdTe layer t_{CdTe}	Deposition time for ZnTe layer t_{ZnTe}	Fraction of Zinc in CZT matrix, 'x'
1	20:80	15.65	84.35	1 min 5 sec	21 sec	0.0567
2	30:70	24.13	75.87	58 sec	32 sec	0.0870
3	40:60	33.10	66.90	51 sec	44 sec	0.1182
4	50:50	42.60	57.40	44 sec	57 sec	0.1510
5	60:40	52.67	47.33	36 sec	1 min 10 sec	0.1865
6	70:30	63.39	36.61	28 sec	1 min 25 sec	0.2210

Table 2 Normalized Nickel contact performance parameters for $Cd_{1-x}Zn_xTe$ 100 nm thin films

Fraction of Zinc in CZT matrix (x)	Metallic Contacts	Ideality Factor (before heating in dark) n_d	Barrier Height (before heating in dark) Φ_{bd}	Contact resistivity (before heating in dark) ρ_d	Ideality Factor (after heating in dark) n_t	Barrier Height (after heating in dark) Φ_{bt}	ρ_{dt} (after heating in dark)	ρ_{dt}/ρ_d
0.1510	Ni	0.5775	0.7273	0.0011	0.8593	0.9880	0.6026	1
0.1865	Ni	0.6127	0.9756	0.4156	0.4762	0.9724	0.2239	0.0010
0.2210	Ni	1	1	1	1	1	1	0.0043

VI. DISCUSSIONS

Results of this paper reveal that $Cd_{1-x}Zn_xTe$ thin films of 1 µm thickness has shown better performance with respect to temperature cycling studies as compared to $Cd_{1-x}Zn_xTe$ thin films of 100 nm thickness for 'x' varying from 0.0567 to 0.2210. From the plots showing the variation of normalized values of contact resistivity, ρ_{dt} vs thermal cycle in dark, comprising increasing and decreasing temperatures from 300°K to 333°K, it is observed that out of all the metallic contacts, e.g. Nickel, Aluminium, Indium, Silver and Copper deposited on all the six different compositions of $Cd_{1-x}Zn_xTe$ 1µm thin films, the forward and return paths of Nickel are the closest to each other in almost all the cases. So, it is inferred that Nickel has the best thermal stability and this is an essential feature for ohmic contact. The reason for Nickel showing good contact on the semiconducting films may be explained due to its higher work function to the tune of 5.1 eV. As Cadmium Zinc Telluride (CZT) has work function to the tune of 5.5 eV it may be mentioned that Nickel has formed low Schottky junction on the semicinducting film and thus it has established ohmic contact. Out of all the plots, showing the variation of normalized values of contact resistivity, ρ_{dt} vs thermal cycle in dark, comprising increasing and decreasing temperatures from 300°K to 333°K, with Nickel as the top metallic contact points on all the compositions of $Cd_{1-x}Zn_xTe$ 1 µm thin films, the forward and return paths of the plots are found to be the closest for 'x' = 0.1865. It is thus evident from this study that out of all the compositions of $Cd_{1-x}Zn_xTe$ 1 µm thin films, the maximum thermal stability for Nickel is found to be at 'x' = 0.1865. Also, from Table 2, it is observed that out of the three compositions of $Cd_{1-x}Zn_xTe$ 100 nm thin films, with Nickel as the metallic contact points, the maximum decrease in the value of the ratio ρ_{dt} / ρ_d is found at 'x' = 0.1865. So, it is evident from this study that Nickel has shown the best thermal stability on $Cd_{1-x}Zn_xTe$ 100 nm thin film, at 'x' = 0.1865.

VII. CONCLUSION

This study infers that Nickel has the best thermal stability on $Cd_{1-x}Zn_xTe$ thin films and the best/optimum composition of both $Cd_{1-x}Zn_xTe$ 1µm and 100 nm thin films for 'x' varying from 0.0567 to 0.2210 with Nickel as the contact points is found to be at 'x' = 0.1865.

ACKNOWLEDGEMENTS

Author is thankful to all the members of Advanced Materials and Solar Photovoltaic Division, School of Energy Studies, Jadavpur University, Kolkata, India for their help and cooperation.

REFERENCES

[1]. B. Ghosh Electrical contacts for II-VI semiconductor devices, *Journal of Microelectronics Engineering*, *86*, 2009, 2187-2206.

[2]. H. Bayhan, A. S. Kavasoglu Exact analytical solution of the diode ideality factor of a pn junction device using Lambert W-function model, *Turk J Phys. 31*, 2007, 7-10.

[3]. M. Chakraborty Tuning Parameters of Metal-Semiconductor Contact and Their Influence in Optical Gain, *International Journal of Engineering Science and Technology*, *3 (8)*, 2011, 6299-6304.

[4]. B. Ghosh, M. J. Carter, R. W. Miles, R. Hill, Correct Evaluation of ohmic contacts to p-CdTe thin films, *Electr. Lett. 29(5)*, 1993, 438-440.

[5]. G. P. Carvar, J. J. Kopanski, D. B. Novotny, R. A. Forman, Specific contact resistivity of metal-semiconductor contacts-a new, accurate method linked to spreading resistance, *IEEE Transactions on Electron Devices. 35*, 1998, 489-497.

[6]. S. Averine, Y. C. Chan, and Y. L. Lam Evaluation of Schottky contact parameters in metal-semiconductor - metal photodiode structures, *Applied Physics Letters. 77(2)*, 2000, 274-276.

[7]. M. Chakraborty A Mathematical Model for Current in Metal-Semiconductor Contact, *International Journal of Engineering Science and Technology*, *3 (6)*, 2011, 4794-4800.

[8]. V. V. Filippov, P. V. Frolov, N. N. Polyakov Measurement of the Metal-Semiconductor Contact Resistance and Control of the Specific Resistance of Semiconductor Films, *Russian Physics*. *46*, 2005, 726-735.

[9]. W. Schocley Research and investigations of inverse epitaxial UHF power transistor, Report No. AL-TOR-64-207, Air Force Atomic Laboratory, Wright-Patterson Air Force Base, Ohio, 1964.

[10]. M. Chakraborty Light Soaking Studies on Metal-Semiconductor Contacts, *International Journal of Engineering Science and Technology*, *3 (7)*, 2011, 5956-5963.

[11]. B. Ghosh D. Sc. Engg thesis, Jadavpur University, Kolkata, India, 2006.

[12]. Weblink:http://stinet.dtic.mil/oai/oai?verb=get Record&metadataPrefix=html&identifier=AD A218730.

[13]. B. Ghosh, S. Purakayastha, P. K. Datta, R. W. Miles, M. J. Carter and R. Hill, Formation of a stable ohmic contact to CdTe thin films through the diffusion of P from Ni-P, *Semicond. Sci. Technol. 10*, 1996, 71-76.

[14]. Weblink:http://www.wipo.int/pctdb/images4/PCT-PAGES/1995/05/95002899.pdf

[15]. V. G. Karpov, D. Shvydka and Y. Roussillon, Physics of CdTe Photovoltaics: from Front to Back**,** Invited talk, MRS Spring Meeting, San Francisco, 2005.

[16]. H. Cordes, R. Schmid-Fetzer, Electrical properties and contact metallurgy of elemental (Cu, Ag, Au, Ni) and compound contacts on p-$Cd_{0.95}Zn_{0.05}Te$, *Semicond. Sci. Technol*, *10*, 1995, 77-86.

[17]. S. K. Cheung, N. W. Cheung,. Extraction of Schottky Diode parameters from forward current-voltage characteristics, *Applied Physics Lett. 49 (2)*, 1986.

[18]. K. W. Boer, Non-ideal diode factors, *Journal of Applied Physics*, 51(8), 1980, 4518-4522.

[19]. L. A. Kelly, Master of Science thesis, Louisiana State University and Agricultural and Mechanical College, 2005.

[20]. D. J. Wagenaar, K. Parnham, B. Sundal, G. Maehlum, S. Chowdhury, D. Meier, T. Vandehei, M. Szawlowski, B. E. Patt, Advantages of Semiconductor CZT for Medical Imaging, *Proc. SPIE.* 2007, 6707.

[21]. E. W. Izaguirre, M. Sun, T. Vandehei, P. Despres, Y. Huang, T. Funk, J. Li, K. Parnham, B, B. E. Pratt and B. H. Hasegawa, IEEE Nuclear Science Symposium Conference Record, 2006.

[22]. C. Kittel, *Introduction to Solid State Physics*, (7th ed, John Willey & Sons, 1996, Ch. 3).

[23]. Sze, S. M. (1981). Physics of Semiconductor devices, (2nd ed, New York , Wiley, 1981, Ch. 8).

[24]. B. Ghosh, Work function Engineering and its applications in ohmic contact fabrication to II-VI semiconductors, *Applied Surface Science*, *254*, 2008, 4908-4911.

[25]. Y. Eisen, I. Mardor, A. Shor, IEEE Trans. Nucl. Sci., *49*, 2002, p-172.

[26]. H. Peng, P. D. Olcott, G. Pratx, A. M. K. Foudray, G. Chinn, C. S. Levin, IEEE Nuclear Science Symposium Conference Record, 2007.

[27]. C. N. Brzymialkiewicz, M. P. Tornai, R. L. McKinley and J. E. Bowsher, IEEE Transactions on Medical Imaging, *24*, 2005, p-7.

[28]. A. Burger, M. Groza, Y. Cui, D. Hillman, E. Brewer, A. Bilikiss, G. W. Wright, L. Li, F. Lu, and R. B. James, *Journal of Electronic Material*, *32*, 2003, p-7.

[29]. T. E. Schlesinger, J. E. Toney, H. Yoon, Y. E. Lee, B. A. Brunett, L. Franks, R. B. James, Cadmium zinc telluride and its use as a nuclear radiation detector material, *Material Science and Engineering*. *32*, 2001, pp. 103-189.

[30]. M. Chakraborty, Optimum Stoichiometry of Cadmium Zinc Telluride Thin Films in the Light of Optical, Structural and Photon Generated Gain Studies, *International Journal of Engineering Science and Technology*, *3 (5)*, 2011, pp- 3798-3806.

[31]. http://www.freepatentsonline.com/5528495